Molecular Plant Pathology

WILEY

Molecular Plant Pathology

ORIGINAL ARTICLE OPEN ACCESS

Regulation of Stomatal Responses to Pathogen and Drought Stress by the F-Box Protein AtSKIP5

Ting Zhang[1,2] | Kang Wang[1,2] | Xinyuan Li[1,2] | Cheng Zhang[1,2] | Kui Wang[1,2] | Huajian Zhang[1,2]

[1]Key Laboratory of Agri-Products Quality and Biosafety (Anhui Agricultural University), Ministry of Education, Hefei, China | [2]Anhui Province Key Laboratory of Crop Integrated Pest Management, Department of Plant Pathology, College of Plant Protection, Anhui Agricultural University, Hefei, China

Correspondence: Huajian Zhang (hjzhang@ahau.edu.cn)

Received: 3 June 2024 | **Revised:** 24 January 2025 | **Accepted:** 26 February 2025

Funding: This work was supported by National Natural Science Foundation of China (Grant No. 32472531, 32302304 and 32072366).

Keywords: apoplastic defence | AtSKIP5 | drought tolerance | F-box proteins | stomatal immunity

ABSTRACT

E3 ubiquitin ligases are major components of the ubiquitination cascade and contribute to the stomatal responses to pathogen and drought stress in plants. The F-box SKP1-Interacting Partners (AtSKIPs) proteins are members of the SCF E3 ubiquitin ligase complexes; however, whether they have any involvement in stomatal movement remains unclear. Here, based on tissue expression profiling, we found that the AtSKIP5 protein was highly expressed in guard cells. Mutation of *AtSKIP5* rendered plants more susceptible to *Pseudomonas syringae* pv. *tomato* (Pst) DC3000 and resulted in a significant impairment in stomatal closure after flg22 and Pst DC3000 treatment. Consistently, lines overexpressing *AtSKIP5* were more resistant to Pst DC3000 infection and exhibited more rapid stomatal closure than did other lines. However, the *AtSKIP5*-overexpressing lines and Col-0 line were similarly resistant to Pst$^-$ (coronatine-deficient mutant) infection and did not exhibit stomatal reopening when exposed to Pst DC3000, a Pst$^-$ strain, or a Pst$^-$ strain accompanied by coronatine (COR) treatment. These results suggest that AtSKIP5-mediated resistance to Pst DC3000 is by controlling stomatal immunity via positive regulation of flg22-triggered stomatal closure and suppression of COR-mediated stomatal reopening. Furthermore, apoplastic immunity was compromised in the *skip5* mutants, as evidenced by lower MAPK phosphorylation levels, less reactive oxygen species (ROS) production, and callose deposition induced by flg22, shifting the response in the pathogenic direction. In addition, the *skip5* mutants evidenced an impairment in stomatal closure induced by abscisic acid (ABA), and a lower survival rate and greater water loss under drought stress, suggesting that AtSKIP5 serves as a positive regulator of drought tolerance via ABA-induced stomatal closure. Our results provide new insights into the importance of the stomatal responses to pathogen and drought stresses that are modulated by AtSKIP5 in *Arabidopsis*.

1 | Introduction

Stomata are formed by pairs of guard cells; stomatal movement regulates gas exchange, transpirational water loss, and plant immunity (Melotto et al. 2006; Arnaud et al. 2023). When initiating pathogenesis, plant-pathogenic bacteria must first enter plant tissues (Melotto et al. 2006). Unlike fungal pathogens, bacteria lack the ability to directly penetrate the plant epidermis; they rely entirely on natural openings, particularly stomata, to enter internal tissues (Melotto et al. 2006). The pattern recognition receptors (PRRs) located in guard cells perceive pathogen-associated molecular patterns (PAMPs), triggering rapid stomatal closure; this is termed stomatal immunity (Wang and Gou 2021). Plants infected with the bacterium *Pseudomonas syringae* pv. *tomato* (Pst) DC3000 sense bacterial PAMPs, such as flg22 (a flagellin peptide) and lipopolysaccharide (LPS), and close the stomata to

Ting Zhang, Kang Wang and Xinyuan Li contributed equally to this study.

limit bacterial entry (Melotto et al. 2006; Wang and Gou 2021). *Arabidopsis* PRR FLS2 perceives flg22, demonstrated by the lack of stomatal closure in *fls2*-mutant plants treated with flg22 (Mez and Boller 2000). To successfully colonise plants, pathogens have evolved a variety of virulence factors that subvert host defences. For example, Pst DC3000 produces the toxin coronatine (COR), which reopens the stomata (Melotto et al. 2006). COR binds to the coronatine-insensitive 1-jasmonate ZIM domain (COI1-JAZ) co-receptor complex and then regulates the expression of three transcription factors (TFs) of the NAC family via the master transcriptional factor MYC2, which hijacks the jasmonic acid (JA) signalling pathway to effectively reopen closed stomata (Spoel and Dong 2008; Du et al. 2014; David et al. 2019; Yan et al. 2009). Once pathogens overcome the surface barriers and enter the interior spaces of leaves, the detection of pathogen invasion by host cells induces rapid strengthening of the cell walls and secretion of a set of antimicrobial molecules into the apoplastic region to suppress pathogen growth; this process is termed apoplastic immunity (Monaghan and Zipfel 2012; Doehlemann and Hemetsberger 2013; Su et al. 2017).

Pathogen infections aside, stomata can be rapidly closed in response to abiotic stresses (Shen et al. 2021; Li et al. 2016; Agurla et al. 2018). Drought is a primary abiotic stress that seriously compromises plant growth and productivity (Tian et al. 2022). Upon drought stress developing, the levels of abscisic acid (ABA) (a key plant hormone) increase dramatically. ABA is thought to be synthesised under water stress conditions at the root or leaf level and acts directly on guard cells to induce stomatal closure (Dou et al. 2021; Agurla et al. 2018). It is widely acknowledged that ABA binds to the pyrabactin-resistance-1/pyrabactin resistance-like/regulatory component of aba (PYR/PYL/RCAR) receptors; the complex then captures protein phosphatases 2C (PP2Cs), in turn activating Snf1-related protein kinases 2 such as the Open Stomata 1 (OST1)/SnRK2.6 (Ding et al. 2015; Guzman et al. 2012; Jossier et al. 2009). In *Arabidopsis*, F-box proteins are involved in ABA-mediated stomatal closure under drought conditions. For instance, the F-box protein Drought Tolerance Repressor 1 (DOR1) involved in ABA biosynthesis affects stomatal closure, thus negatively regulating plant drought tolerance (Zhang et al. 2008). The F-box protein RCAR3 Interacting F-box Protein 1 (RIFP1) negatively regulates drought resistance and the expression levels of ABA pathway-related genes (Li et al. 2015). Mutant plants defective in ABA biosynthesis and ABA responses are impaired in terms of both stomatal closure and drought tolerance (Jossier et al. 2009; Li et al. 2015, 2016; Dou et al. 2021; Zhang et al. 2008; Ding et al. 2015).

The ubiquitin (Ub) 26S proteasome pathway controls the degradation of many proteins and thus modulates many fundamental cellular and physiological processes (Rao et al. 2018; Jennifer et al. 2002). Ub conjugation is achieved via an ATP-dependent reaction cascade involving the sequential actions of three enzymes: E1 Ub-activating enzymes, E2 Ub-conjugating enzymes, and E3 Ub ligases (Jennifer et al. 2002). Of the E3 Ub ligases, the SCF complex contains SKP1, CULLIN1 (CUL1)/CDC53, the ring finger protein RING-box 1, and F-box proteins (Varshney et al. 2023; Rao et al. 2018; Hong et al. 2017; Naeem-ul-Hassan et al. 2017). Increasing evidence suggests that E3 Ub ligases regulate stomatal movement during the plant cell response to diverse stresses. For example, the E3 Ub ligase MREL57 modulates microtubule stability and stomatal closure in response to ABA (Dou et al. 2021). RZFP34/CHYR1, a RING E3 Ub ligase, regulates stomatal movement and drought tolerance via OST1/SnRK2.6-mediated phosphorylation (Ding et al. 2015). The RING E3 Ub ligase JUL1 participates in ABA-mediated microtubule depolymerisation and stomatal closure (Yu et al. 2020). Thus, the identification of the E3 Ub ligases involved in stomatal movement would boost our understanding of the mechanisms underlying stomata-regulated plant adaptations.

F-box proteins are subunits of the SCF complexes that regulate many cellular processes, including the cell cycle transition, transcriptional regulation, and signal transduction (Varshney et al. 2023; Hirofumi et al. 2002; Jennifer et al. 2002; Rao et al. 2018). The *Arabidopsis thaliana* genome encodes at least 700 F-box proteins (Varshney et al. 2023; Jennifer et al. 2002). The SKP1/ASK-Interacting proteins (SKP1-Interacting Partners [AtSKIPs]) may bind to S-phase kinase-associated protein 1 (SKP1/ASK1) via the F-box domain (Hong et al. 2017; Varshney et al. 2023; Naeem-ul-Hassan et al. 2017). However, the functions of several AtSKIPs and the effects of AtSKIPs remain to be elucidated under stress. In this study, we show that the F-box protein AtSKIP5 is involved in resistance to Pst DC3000 by controlling both stomatal immunity and apoplastic immunity. In addition, AtSKIP5 positively regulates the drought tolerance associated with ABA-induced stomatal closure. Our results emphasise the importance of the F-box protein AtSKIP5 not only in terms of pathogen infection but also during drought stress and provide evidence of stomatal responses to pathogen and drought stresses.

2 | Results

2.1 | Identification and Analysis of AtSKIP Proteins in *Arabidopsis thaliana*

To investigate the characteristics of AtSKIPs proteins, all AtSKIPs protein sequences in *A. thaliana* were obtained from the Phytozome and the TAIR databases. After confirming these sequences through reciprocal searches in the NCBI CD database, 26 AtSKIPs proteins were isolated, including 11 AtSKIPs proteins containing the F-box domain and 15 AtSKIPs proteins lacking the F-box domain. Because these 15 AtSKIPs proteins lacked the typical F-box domain, they were not classified as F-box proteins. Ultimately, 11 AtSKIPs proteins containing the F-box domain were selected for further analysis. Figure 1 shows the phylogenetic relationships, motifs, and the schematic protein structures of the *Arabidopsis* AtSKIPs. Phylogenetic analysis indicated that these proteins could be classified in terms of their structural domains into five types (Figure 1A). To investigate motifs shared by the AtSKIPs, we used the MEME motif search tool and mapped the results using TBtools (Chen et al. 2020). Ten conserved motifs were determined. Motif analysis showed that 11 AtSKIPs encoded motif 1 (WSELPPDLLDLIANR); the exception was AtSKIP18 (Figure 1A, middle). Based on the protein conserved domain analysis conducted using the NCBI Conserved Domain Search Database and TBtools, it was shown that only AtSKIP5 and AtSKIP18 exclusively contained the F-box domain, whereas the other AtSKIP proteins possessed additional domains (AMN1, PRK14131, PHA03098, Kelch_1,

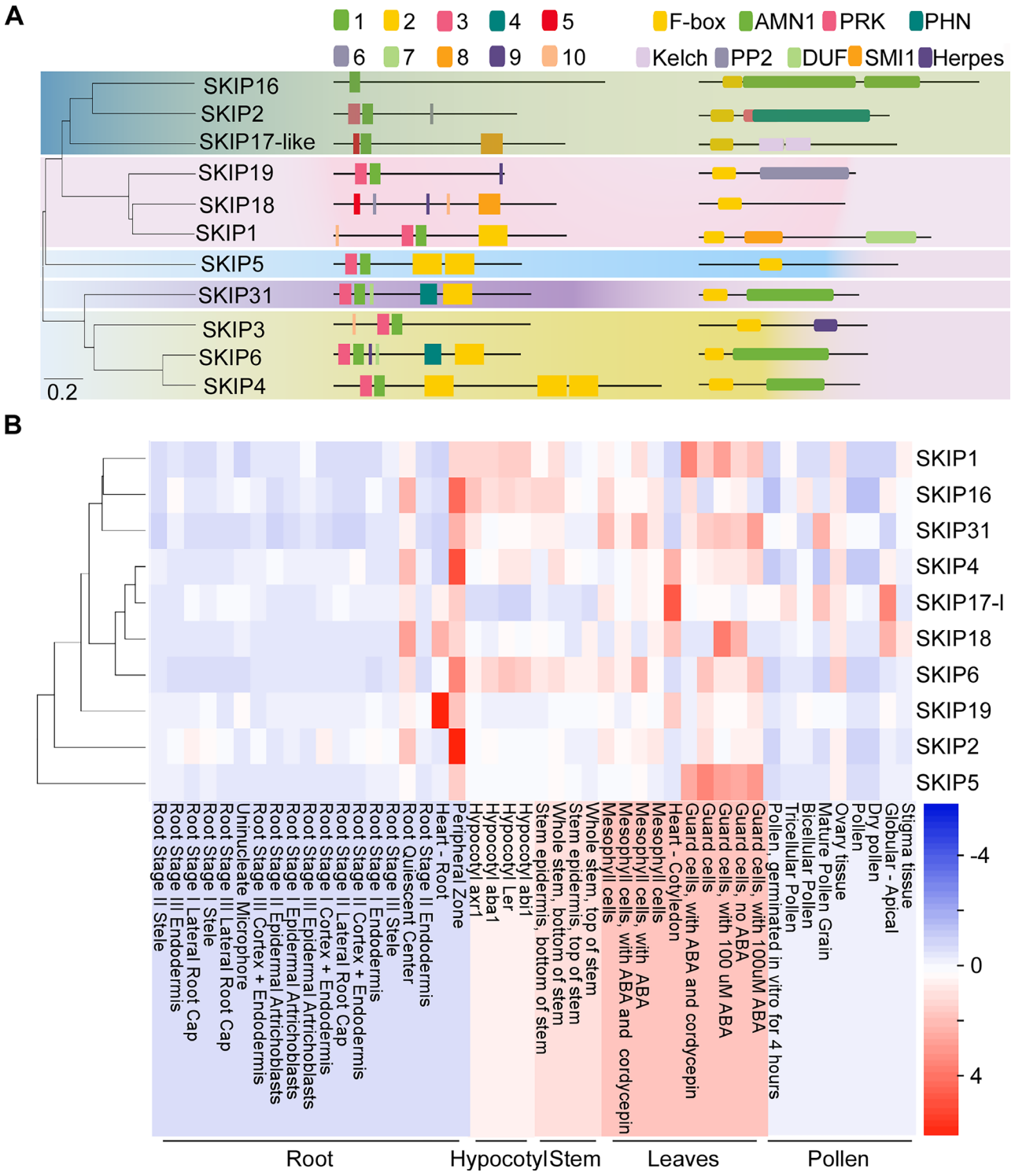

FIGURE 1 | Identification and analysis of AtSKIPs proteins in *Arabidopsis thaliana*. (A) Phylogenetic analysis, motifs and protein structures of AtSKIPs. A phylogenetic tree was constructed in MEGA 11 using the neighbour-joining method with 1000 bootstrap replicates based on the full-length amino acid sequences of 11 AtSKIPs proteins aligned with ClustalW. The motif patterns were predicted using the MEME database (https://meme-suite.org/meme/tools/meme). The domain predicted using the NCBI CD database (https://www.ncbi.nlm.nih.gov/Structure/bwrpsb/bwrpsb.cgi). These results were mapped by TBtools. AtSKIP1: AT5G57900; AtSKIP2: AT5G67250; AtSKIP3: AT2G02350; AtSKIP4: AT3G61350; AtSKIP5: AT3G54480; AtSKIP6: AT2G21950; AtSKIP16:AT1G06110; AtSKIP17-like protein: AT4G02735; AtSKIP18: AT4G08980; AtAtSKIP19: AT4G05460; AtSKIP31: AT5G45360. (B) The tissue expression profile of the AtSKIPs. The expression data for each AtSKIPs family member were extracted from the Arabidopsis eFP Browser. The expression data is shown as a heatmap using the HEATMAP tools (http://www.heatmapper.ca/).

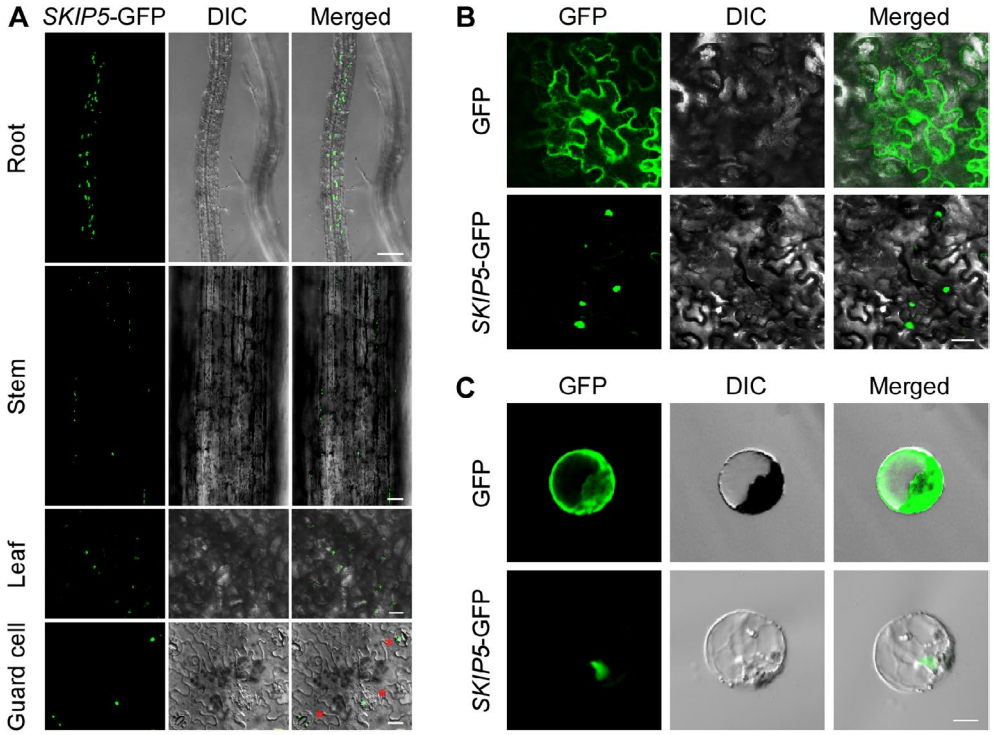

FIGURE 2 | AtSKIP5 is expressed in guard cells. (A) Expression of *Arabidopsis* transgenic seedlings with the AtSKIP5-GFP driven by the native promoter. Two-week-old seedlings of the transgenic line were used for imaging. Scale bar (guard cell/leaf/stem/root) = 20/100/50/200 μm. (B) Localisation of AtSKIP5-GFP fusion in *Nicotiana benthamiana*. pBINPLUS- GFP was used as a negative control. Scale bar = 50 μm. (C) Localisation of AtSKIP5-GFP fusion in Col-0 mesophyll protoplasts. pUC19-GFP was used as a negative control. Scale bar = 50 μm.

PP2, DUF525, SMI1 and Herpes_UL92) besides the F-box (Figure 1A).

Different tissues vary in terms of function (Gautam and Sarkar 2015). To explore the tissue expression of *AtSKIPs* genes, the expression datasets of the *AtSKIPs* from 46 tissues/organs in the *Arabidopsis* eFP Browser Database (http://bbc.botany.utoronto.ca/efp/cgi-bin/efpWeb.cgi) were analysed. Unfortunately, information on AtSKIP3 was unavailable in the database. Given that AtSKIP5 and AtSKIP18 exclusively contained a single domain, the F-box domain, amongst the other AtSKIPs proteins, their expression in different tissues was monitored. AtSKIP18 was expressed in various tissues, including roots, leaves, and pollen, while AtSKIP5 was highly expressed in guard cells (Figure 1B). Therefore, we focused on the function of AtSKIP5 for further study.

2.2 | AtSKIP5 Is Expressed in Guard Cells

AtSKIP5 (AT3G54480) encodes a 274-amino acid (aa) F-box protein containing a characteristic F-box domain at the N terminus (aa 38–79). A search of the NCBI CD database (https://www.ncbi.nlm.nih.gov/Structure/cdd/) suggested that AtSKIP5 is a component of the SCF E3 Ub ligase complexes, which can interact with SKP1/ASK1. To investigate the interaction between AtSKIP5 and AtASK1 in *Arabidopsis*, a yeast two-hybrid (Y2H) assay was performed. The results displayed that yeast cells co-transformed with AtASK1-AD and AtSKIP5-BD were capable of growth on the selective medium (SD − A/H/T/L), suggesting that AtSKIP5 interacts with AtASK1 within the Y2H system. To further confirm the interaction between AtSKIP5 and AtASK1 proteins, a bimolecular fluorescence complementation (BiFC) assay was employed, yielding consistent results (Figure S1F,G). A stable transgenic *Arabidopsis* line expressing *AtSKIP5*-GFP driven by the native promoter was used to assess the expression pattern of AtSKIP5. Punctate GFP signals were observed in the stems, leaves, and roots. Interestingly, GFP signals were most pronounced in the guard cells of the epidermis at the cellular level (Figure 2A). Next, the subcellular localisation of AtSKIP5 was examined by transient expression using *Arabidopsis* mesophyll protoplasts and *Nicotiana benthamiana* leaves. Confocal microscopy showed that the GFP fluorescence signal was predominantly concentrated in the nucleus (Figure 2B,C). These findings suggested that the nuclear-localised protein AtSKIP5 was expressed in the vegetative tissues, including the guard cells.

2.3 | AtSKIP5 Positively Regulates Pst DC3000- and flg22-Induced Stomatal Closure

To investigate the possible function of AtSKIP5, two T-DNA insertion mutant lines (SALK_055942 and SALK_044720) were obtained. The *skip5* mutations were inserted in the untranslated region (UTR) and the second exon 742 bp downstream of the ATG start site, respectively, and reverse transcription-quantitative PCR (RT-qPCR) showed that the transcriptional expression level of *AtSKIP5* in *skip5* mutants was lower compared to that of Col-0 (Figure S1A,B,C,E). Next, three *AtSKIP5*-overexpressing lines (OE-16#, OE-17#, and OE-19#) were generated. The transcriptional expression levels of *AtSKIP5* in the OE-17# and OE-19# lines were higher than those in Col-0, as revealed by RT-qPCR.

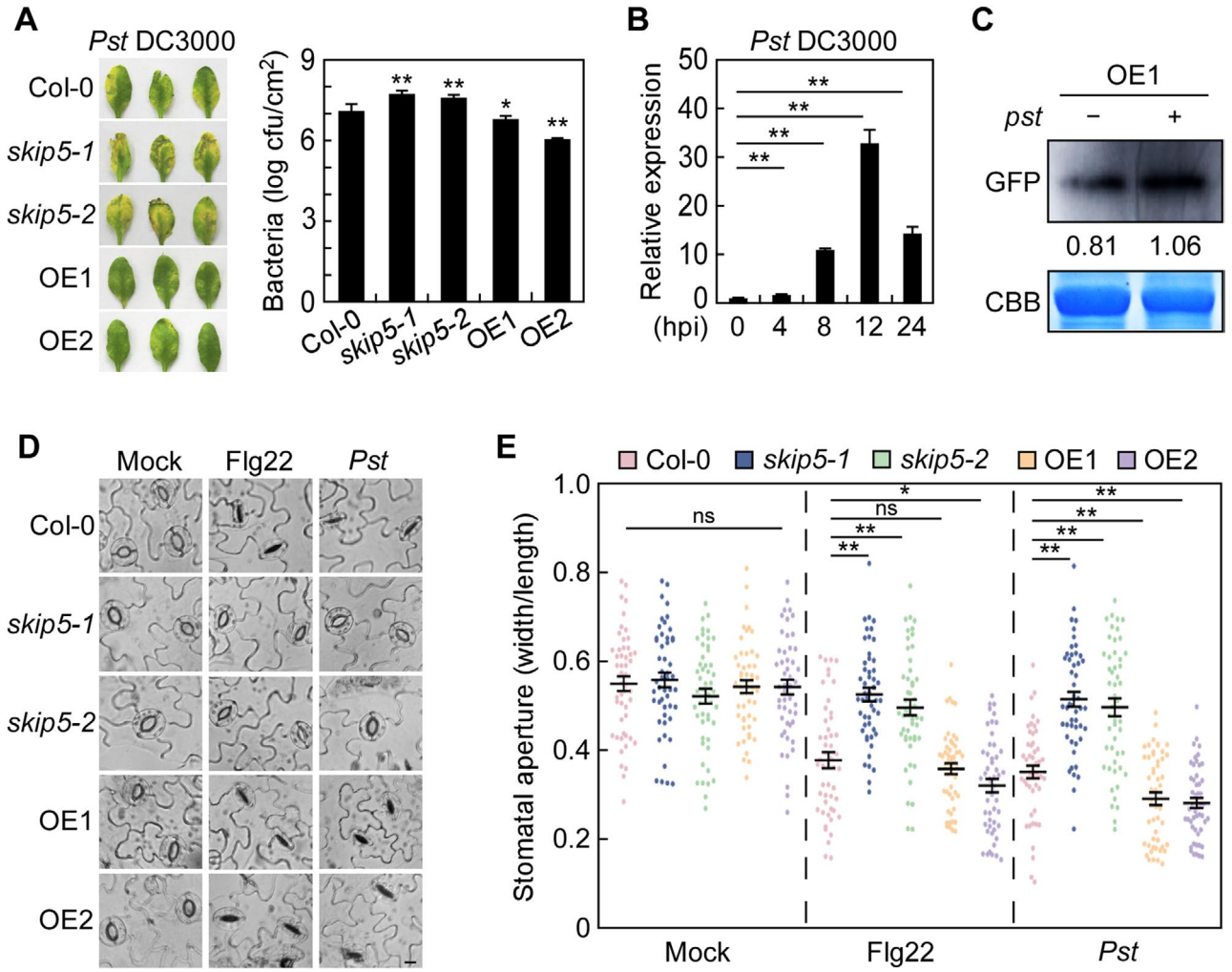

FIGURE 3 | AtSKIP5 is required for *Pseudomonas syringae* pv. *tomato* (Pst) DC3000- and flg22-induced stomatal closure. (A) The disease symptoms and titres of 5-week-old Col-0, *skip5-1, skip5-2* mutant, OE1 and OE2 plants were evaluated after dip-inoculation with Pst DC3000 (10^7 cfu/mL) and photographed at 3 days after inoculation (dai). Error bars of bacterial titres analysis are SD of three biological replicates. Asterisks indicate significant differences by two-tailed Student's *t* test using GraphPad Prism 8.0.1 at $p < 0.01$ (**) or $p < 0.05$ (*). (B) Reverse transcription-quantitative PCR analyses of the expression levels of *AtSKIP5* in Col-0 after dip-inoculation with Pst DC3000 (10^7 cfu/mL) at different times. Error bars are SD of three biological replicates. Statistical analysis was performed by one-way ANOVA with Tukey HSD using GraphPad Prism v. 8.0.1, and asterisks represents significant differences at $p < 0.01$ (**). (C) Western blot analysis of the AtSKIP5-GFP with (+) or without (–) dip-inoculation of Pst DC3000 using anti-GFP antibodies. Relative GFP intensity was analysed by ImageJ. (D and E) Stomatal closure upon Pst DC3000 inoculation and flg22 treatment. Epidermal peels of 5-week-old plants were floated in a suspension of Pst DC3000 and flg22 in stomatal buffer. Scale bar = 50 μm. Error bars are SE of three biological replicates, each consisting of 50 stomata from three plants. Statistical analysis was performed by one-way ANOVA with Tukey HSD using GraphPad Prism v. 8.0.1, and asterisk represents significant differences at $p < 0.01$ (**) or $p < 0.05$ (*).

The results of western blotting further supported these findings (Figure S1D,E). Therefore, OE-17# (OE1) and OE-19# (OE2) were chosen for further studies.

To evaluate the potential role of AtSKIP5 in terms of bacterial resistance, the *skip5* mutant lines (*skip5-1* and *skip5-2*) and the *AtSKIP5*-overexpressing lines (OE1 and OE2) were dip-inoculated with Pst DC3000. The *skip5* mutants exhibited stronger bacterium-mediated yellowing and wilting and increased bacterial titres at 3 days after inoculation (dai) compared to the Col-0. However, OE1 and OE2 were more resistant to Pst DC3000 infection (Figure 3A). RT-qPCR analysis showed that the transcriptional expression levels of *AtSKIP5* were significantly higher after dip-inoculation with Pst DC3000 compared to the mock (0 h), especially at 12 h post-inoculation (hpi) (Figure 3B). Western blot analysis revealed that the AtSKIP5-GFP level was higher after dip-inoculation with Pst DC3000 than in controls (Figure 3C). These results suggest that functional AtSKIP5 is required for resistance to Pst DC3000. As AtSKIP5 is located in guard cells, we next tested whether the AtSKIP5 resistance to Pst DC3000 is associated with bacterium-induced stomatal closure. The stomatal aperture assay was performed after Pst DC3000 inoculation. For these experiments, *Arabidopsis* leaves were exposed to stomatal buffer and light-adapted for at least 2 h to ensure that most of the stomata were open before Pst DC3000 inoculation. The epidermal peels of the Col-0 plants exhibited rapid closure at 1.5 h after Pst DC3000 inoculation, consistent with previous findings (Chan et al. 2020). Stomatal closure was not observed in the *skip5* mutants, but the stomata of the *AtSKIP5*-overexpressing lines demonstrated

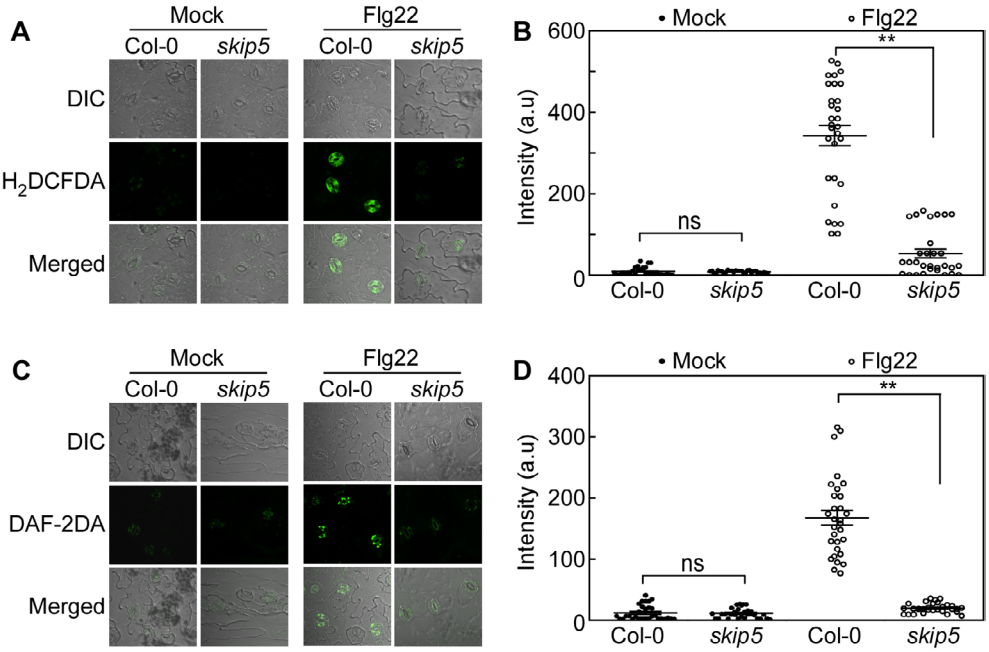

FIGURE 4 | Mutation of *AtSKIP5* compromises flg22-triggered reactive oxygen species (ROS) and nitric oxide (NO) production in guard cells. (A) ROS accumulation in guard cells. Epidermal peels of 5-week-old plants were floated in stomatal buffer containing flg22 and then stained with 50 mM H_2DCF-DA. Scale bar = 50 μm. (B) The fluorescence intensity was statistically analysed using ImageJ. Error bars are SD of 30 guard cells. Asterisks indicate significant differences by two-tailed Student's *t* test using GraphPad Prism v. 8.0.1 at $p < 0.01$ (**) . (C) NO production in guard cells. Epidermal peels of 5-week-old plants were floated in stomatal buffer containing flg22 and then stained with 50 mM DAF-2DA. Scale bar = 50 μm. (D) The fluorescence intensity was statistically analysed using ImageJ. Error bars are SD of 30 guard cells. Asterisks indicate significant differences by two-tailed Student's *t* test using GraphPad Prism v. 8.0.1 at $p < 0.01$ (**).

more closure than did those of Col-0 (Figure 3D). Statistical analysis of stomatal aperture data after Pst DC3000 inoculation supported these findings (Figure 3E). Flg22, a Pst DC3000 PAMP, induced plant stomatal closure to limit bacterial entry; this has been well documented. To explore the role played by AtSKIP5 in PAMP-induced stomatal closure, stomatal aperture assays were performed after all plants were treated with flg22. The stomata of the *AtSKIP5*-overexpressing lines exhibited more marked closure than those of Col-0 and the mutants were still open after treatment with flg22 for 1.5 h, similar to what was seen after Pst DC3000 treatment (Figure 3D,E). In addition, the stomatal aperture of OE1 was significantly smaller than that of Col-0 only after treatment with Pst DC3000, but the stomatal aperture of OE2 was smaller than that of Col-0 after treatment with Pst DC3000 or flg22 (Figure 3E). Taken together, these results suggest that AtSKIP5 positively regulates Pst DC3000- and flg22-induced stomatal closure.

2.4 | Mutation of *AtSKIP5* Compromises flg22-Triggered Reactive Oxygen Species and Nitric Oxide Production in Guard Cells

Accumulations of reactive oxygen species (ROS) and nitric oxide (NO) in guard cells are amongst the earliest hallmarks of stomatal closure in response to flg22 (Sierla et al. 2016; Arnaud et al. 2023). To explore whether AtSKIP5 affects the accumulation of ROS and NO under flg22 treatment, the production of ROS and NO in guard cells was examined with the fluorescein probes H_2DCFDA and DAF-2DA, respectively. In the mock treatment, almost no ROS production was detected in Col-0 and the *skip5-1* mutant. However, fluorescence observations showed that flg22 rapidly induced the production of ROS in guard cells of Col-0 and the mutant, and ROS production triggered by flg22 in the *skip5-1* mutant was significantly less than that of Col-0 (Figure 4A,B), indicating that AtSKIP5 was involved in flg22-triggered ROS production. Next, the production of NO was also examined. The *skip5-1* mutant exhibited no significant change in NO production compared to Col-0 in mock-treated plants, similar to what was seen when ROS production was examined in mock-treated plants. However, compared to Col-0, the *skip5-1* mutant exhibited an obvious decrease in NO production on treatment with flg22 (Figure 4C,D). These results suggested that AtSKIP5 affected flg22-induced ROS and NO production in guard cells.

2.5 | AtSKIP5 Suppresses Coronatine-Dependent Stomatal Reopening

Coronatine (COR) contributes to the virulence of Pst DC3000 in *Arabidopsis*, to reopen stomata to allow bacterial entry (Guo et al. 2018). To investigate whether AtSKIP5 was involved in the stomatal defence to Pst DC3000 by regulating COR-dependent stomatal reopening, a stomatal aperture assay was performed using COR-deficient mutant bacteria (Pst DC3000 COR^-, Pst^-). The stomata of Col-0 were closed after Pst DC3000 and Pst^- treatment for 1.5 h, consistent with previous findings (Melotto et al. 2006); OE1 and OE2 exhibited more rapid stomatal closure than did Col-0 (Figure 5A,B). The stomata of Col-0 plants remained closed for up to 4 h after Pst^- treatment, but they were dramatically reopened after Pst

DC3000 treatment and Pst⁻ accompanied by COR treatment (Figure 5A,B). These results indicated that COR played a key role in *Arabidopsis* stomatal reopening. However, the stomata of OE1 and OE2 plants remained closed after treatment with Pst DC3000, Pst⁻, and Pst⁻ accompanied by COR (Figure 5A,B). These results indicate that AtSKIP5 suppressed COR-induced stomatal reopening. To further define the involvement of COR in bacterial-induced stomatal defence, Pst⁻ was employed to test COR-dependent virulence. After dip inoculation with Pst⁻, the resistance of *AtSKIP5*-overexpressing plants was similar to that observed in Col-0 after bacterial treatment, indicating that AtSKIP5 plays a role in stomatal defence against

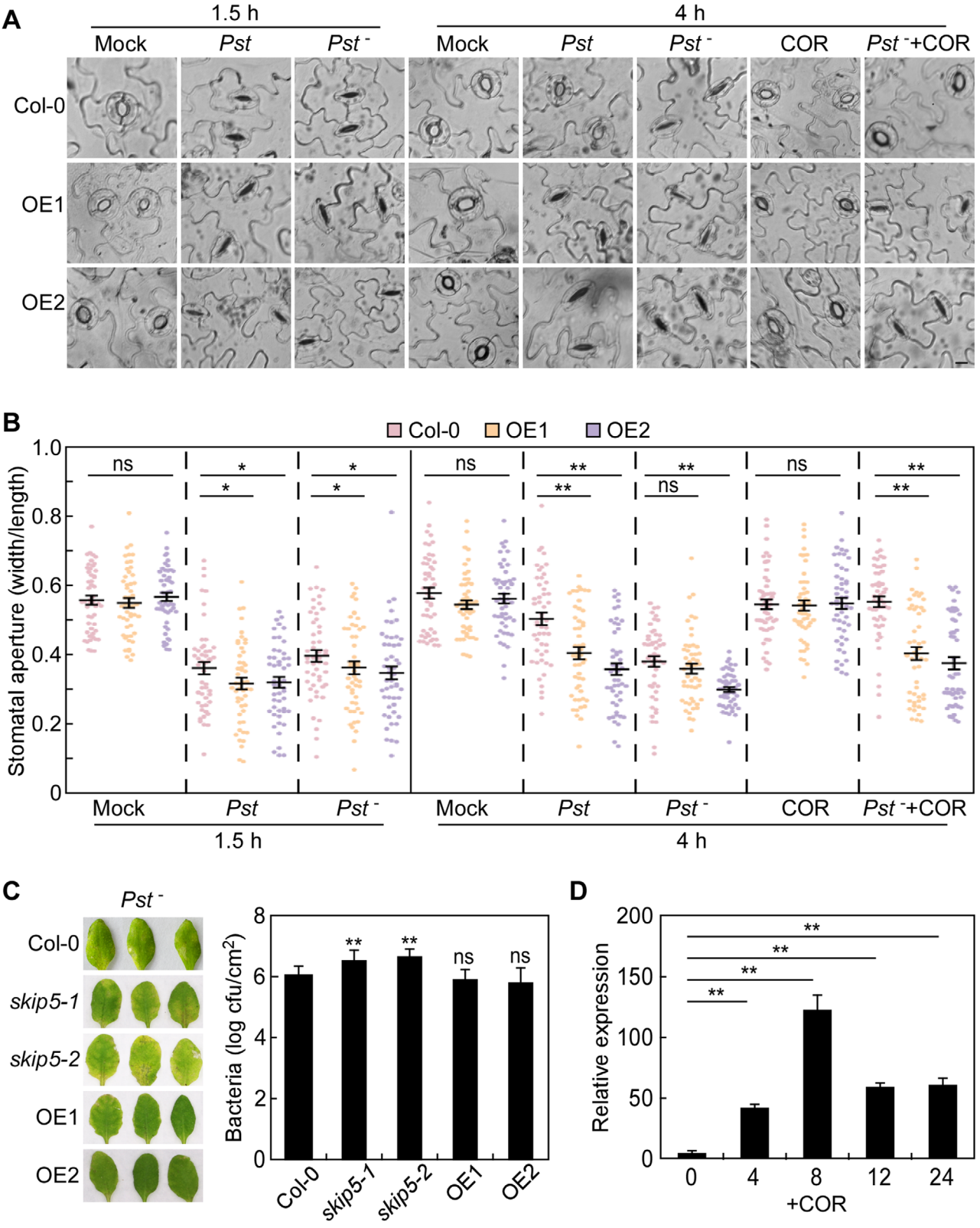

FIGURE 5 | Legend on next page.

FIGURE 5 | AtSKIP5 suppresses coronatine (COR)-dependent stomatal reopening. (A and B) Stomatal aperture was examined upon *Pseudomonas syringae* pv. *tomato* (Pst) DC3000, Pst⁻, COR and Pst⁻ with COR treatment. Epidermal peels of 5-week-old plants were floated in stomatal buffer containing different treatment. Error bars are SE of three biological replicates, each consisting of 50 stomata from three plants. Statistical analysis was performed by one-way ANOVA with Tukey HSD using GraphPad Prism v. 8.0.1, and asterisk represents significant differences at $p < 0.01$ (**) or $p < 0.05$ (*). Scale bar = 20 μm. (C) The disease symptoms and titres of 5-week-old Col-0, *skip5-1, skip5-2*, OE1 and OE2 plants were evaluated after dip inoculation with Pst⁻ (10^7 cfu/mL) and photographed at 4 days after inoculation (dai). Error bars of bacterial titres analysis are SD of three biological replicates, each with three plants ($n = 15$). Asterisks indicate significant differences by two-tailed Student's *t* test using GraphPad Prism v. 8.0.1 at $p < 0.01$ (**). (D) Reverse transcription-quantitative PCR analyses of the expression levels of *AtSKIP5* in Col-0 after treatment with 0.5 ng/mL COR at different time. Error bars are SD of three biological replicates. Statistical analysis was performed by one-way ANOVA with Tukey HSD using GraphPad Prism v. 8.0.1, and asterisk represents significant differences at $p < 0.01$ (**).

Pst DC3000 by involvement in COR-induced stomatal reopening. Surprisingly, the *skip5* mutants were associated with more disease symptoms and significantly greater pathogen growth than were Col-0 (Figure 5C). We measured the gene expression levels of *AtSKIP5* after COR treatment and found that *AtSKIP5* was highly expressed after COR treatment, particularly at 8 h (Figure 5D), suggesting that COR activated AtSKIP5 expression. Next, the transcriptional expression levels of COR-related genes were analysed by RT-qPCR in Col-0, *skip5* mutant and OE2 plants at 8 h after Pst DC3000 infection. The results showed that the transcriptional expression levels of *AtANAC019*, *AtANAC055* and *AtANAC072* in the *skip5-1* mutant were significantly increased compared to Col-0 after Pst DC3000 infection, while the expression levels of *AtCOI1* and *AtMYC2* did not show significant change in the *skip5-1* mutant compared to Col-0 (Figure S2A). To explore how AtSKIP5 affects AtANACs, the protein expression levels of these three AtANACs proteins were examined in protoplasts of Col-0 and the *skip5-1* mutant. The result showed that the intensity of AtANAC019/ANAC055/ANAC072-GFP was greater in the *skip5-1* mutant compared to that in Col-0 (Figure S2B). These data suggested that AtSKIP5 may suppress COR-induced stomatal reopening by facilitating the degradation of three AtANAC proteins.

COR is a structural mimic of jasmonic acid-isoleucine (JA-Ile) that hijacks the JA signalling pathway to suppress plant defences (Du et al. 2014). Accumulation of JA inhibits plant root growth; this is a common phenomenon. To investigate whether AtSKIP5 regulated JA signalling, the root lengths of AtSKIP5 treated with different concentrations of MeJA were evaluated. The root growth inhibition rates were similar in the *skip5* mutant and Col-0 seedlings upon treatment with 2.5 mM MeJA, but they were about 14% greater in the *skip5* mutant than in Col-0 seedlings on treatment with 5 mM MeJA. In contrast, OE2 seedlings had longer roots than Col-0 seedlings on treatment with either 2.5 or 5 mM MeJA (Figure S3A–C). These results indicated that AtSKIP5 promotes root growth by inhibiting JA signalling. Next, the gene expression level of *AtSKIP5* was examined at different times after treatment with 5 mM MeJA. The *AtSKIP5* gene was significantly induced under MeJA treatment compared to the control, especially at 12 h (Figure S3D). *PDF1.2* expression was blocked in the JA response mutant *coi1-1*; this served as a marker gene of JA signalling (Penninckx et al. 1998). The gene expression levels of *PDF1.2* in Col-0, OE1, and OE2 plants were also analysed. The gene expression level of *PDF1.2* was significantly decreased in OE1 and OE2 plants compared to the Col-0 plant (Figure S3E), implying that AtSKIP5 negatively regulated JA signalling.

2.6 | AtSKIP5 Is Involved in the Apoplastic Defence Against Pst DC3000

Stomatal closure is only one of several functional outputs induced by PAMPs, and the plant apoplast is often a battleground for plant–microbe interactions (Zeng et al. 2011). Therefore, a possible effect of AtSKIP5 on the PAMP-triggered apoplastic defence, which uses flg22, was investigated. The resistance of Col-0, the *skip5* mutants, and the *AtSKIP5*-overexpressing lines after infiltrative inoculation with Pst DC3000 was evaluated. Before inoculation with Pst DC3000, all plants were pretreated with 100 nM flg22 or water (mock treatment) for 24 h. The results showed that all plants that were pretreated with flg22 exhibited significantly smaller bacterial populations than plants pretreated with water. However, the *skip5* mutants were more susceptible to bacteria than the Col-0 plants pretreated with either flg22 or water, whereas the *AtSKIP5*-overexpressing lines exhibited the opposite effects (Figure 6A). These results suggested that AtSKIP5 was not only involved in the basal apoplastic defence but also the apoplastic defence induced by flg22 against Pst DC3000.

To evaluate whether AtSKIP5 played a role in early apoplastic PTI, ROS production and MAPK phosphorylation levels were evaluated. The ROS burst in *AtSKIP5*-overexpressing plants was more pronounced than that in Col-0 plants after treatment with flg22, but the ROS burst in the *skip5* mutant was much weaker than that of Col-0 (Figure 6B). In terms of the MPK3 and MPK6 phosphorylation levels, the mutant *skip5-1* exhibited lower MPK3/MPK6 activation levels than the Col-0 plant after treatment with flg22 (Figure 6C). To examine whether AtSKIP5 played a role in the late PAMP-triggered immunity (PTI) responses, the gene expression levels of the PTI-responsive genes *FRK1* and *CYP81F2* in Col-0, the *skip5* mutants, and overexpressing plants were analysed at 24 h after the infiltration with Pst DC3000. Although the gene expression levels of *FRK1* and *CYP81F2* in *AtSKIP5*-overexpressing plants were decreased compared to Col-0 under normal conditions (0 h), they did not differ significantly from those of the Col-0 plant after the infiltration with Pst DC3000 (Figure 6D). Callose deposition was less marked in the *skip5* mutants than in Col-0 plants treated with flg22, and it was significantly higher in OE2 than in Col-0 plants (Figure 6E). Collectively, these results indicate that AtSKIP5 is involved in apoplastic

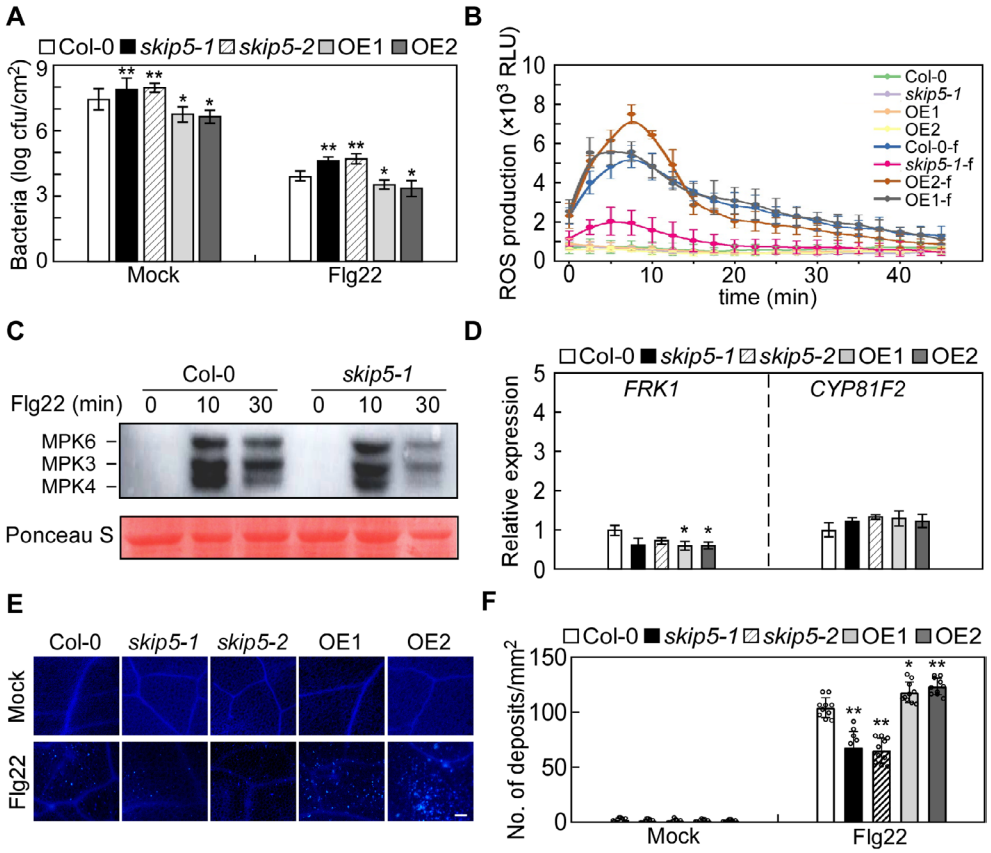

FIGURE 6 | AtSKIP5 is involved in apoplastic defence against *Pseudomonas syringae* pv. *tomato* (Pst) DC3000. (A) The bacterial titres analysis of 5-week-old Col-0, *skip5-1, skip5-2*, OE1 and OE2 plants were evaluated after infiltration with Pst DC3000 (10^5 cfu/mL) following pretreatment with 100 nM flg22 or water (Mock) for 24 h. (B) Production of reactive oxygen species (ROS). Leaf discs were collected from 5-week-old *Arabidopsis* Col-0, *skip5-1* mutant, OE1 and OE2 plants. The luminescence was measured over time after treatment with control solution or 100 nM flg22. Relative light units (RLUs) were evaluated at the indicated time points. Error bars are SD from three independent experiments each with at least 12 leaf discs ($n \geq 36$). (C) MAPK activation. 3-week-old *Arabidopsis* seedlings from Col-0 and *skip5-1* mutant plants were infiltrated with 0.1 μM flg22. MAPK activation was analysed by anti-phosphor-p44/42 MAK kinase immunoblotting. Experiments were repeated three times with similar results. (D) Reverse transcription-quantitative PCR analyses of the expression levels of *FRK1* and *CYP81F2* in Col-0 *skip5-1, skip5-2*, OE1 and OE2 plants after infiltration-inoculation with Pst DC3000 (10^5 cfu/mL) at 24 h. Error bars are SD of three biological replicates. Asterisks indicate significant differences by two-tailed Student's *t* test using GraphPad Prismv. 8.0.1 at $p < 0.05$ (*). (E) Callose deposition upon flg22 treatment. Five-week-old plants were infiltrated with 1 μM flg22 or water (Mock). After 24 h, leaf discs from Col-0, *skip5-1, skip5-2*, OE1 and OE2 lines were stained with aniline blue and observed under a microscope. Scale bar = 20 μm. (F) The number of callose deposition were quantitative analysis. Error bars are SD of three biological replicates. Asterisks indicate significant differences by two-tailed Student's *t* test using GraphPad Prism v. 8.0.1 at $p < 0.01$ (**).

defence, playing critical roles in early apoplastic PTI and callose deposition.

2.7 | AtSKIP5 Positively Regulates ABA-Induced Stomatal Closure and Drought Tolerance

ABA is the best-known hormone that promotes stomatal closure; the effects of AtSKIP5 on ABA-induced stomatal closure were therefore tested. First, the gene expression levels of *AtSKIP5* were assessed in Col-0 seedlings treated with ABA for different times. The ABA-responsive gene *AtRD29A* served as a positive control. As the ABA treatment time increased, the gene expression levels of *AtSKIP5* gradually rose (Figure 7A), suggesting that ABA positively regulates the expression of *AtSKIP5*. Next, the stomatal aperture assay was performed to explore the effects of AtSKIP5 on ABA-induced stomatal closure. The stomata of *AtSKIP5*-overexpressing lines closed more rapidly than those of the Col-0 plant, but the stomata of the mutant were still open after treatment with ABA for 1.5 h (Figure 7B). Statistical analysis of the stomatal aperture ratios further supported these findings (Figure 7C). These results suggested that AtSKIP5 was required for ABA-induced stomatal closure.

ABA-mediated stomatal conductance helps prevent water loss through transpiration and plays a crucial role in drought response. Given that AtSKIP5 is involved in ABA-induced stomatal closure, the role of AtSKIP5 in drought was examined. Firstly, we compared the ability of plants to avoid water loss by analysing the differences in survival amongst all plants growing under water-deficient conditions. The Col-0 and *AtSKIP5*-overexpressing lines remained turgid, and the leaves remained green after the soil was allowed to dry for 14 days, whereas the *skip5* mutant seedlings exhibited severe wilting and chlorosis of the rosette leaves (Figure 7D). A statistical

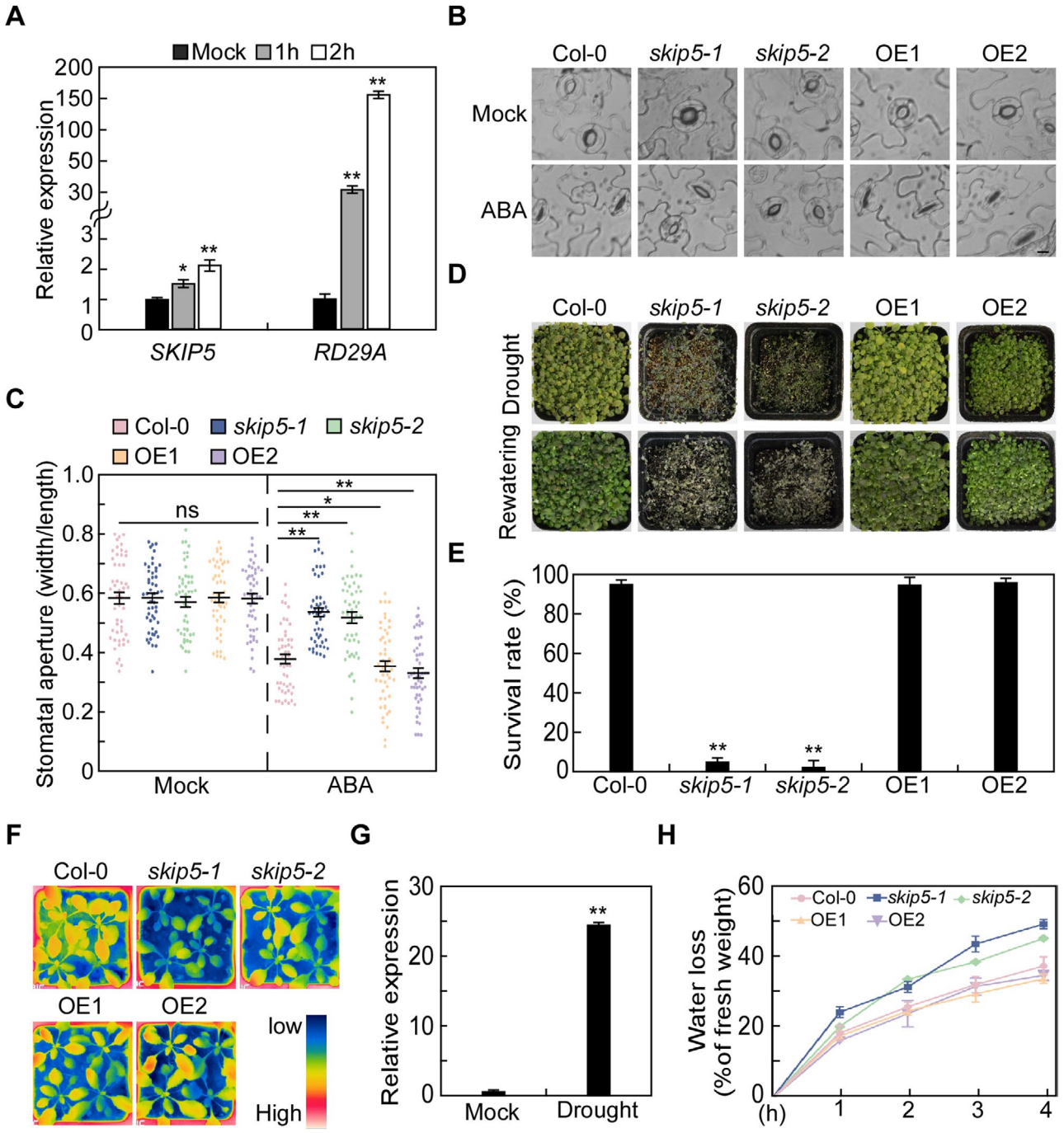

FIGURE 7 | AtSKIP5 positively regulates abscisic acid (ABA)-induced stomatal closure and drought tolerance. (A) Reverse transcription-quantitative PCR (RT-qPCR) analysis of the expression levels of *AtSKIP5* and *RD29A* in Col-0 after various treatment durations using 10 μM ABA. Error bars are SD of three biological replicates. Asterisks indicate significant differences by two-tailed Student's *t* test using GraphPad Prism v. 8.0.1 at $p < 0.01$ (**) or $p < 0.05$ (*). (B and C) Stomatal closure upon treat with 10 μM ABA. Epidermal peels of 5-week-old plants were floated in a suspension of ABA in stomatal buffer. Scale bar = 20 μm. Error bars are SE of three biological replicates, each consisting of 50 stomata from three plants. Statistical analysis was performed by one-way ANOVA with Tukey HSD using GraphPad Prism v. 8.0.1, and asterisk represents significant differences at $p < 0.01$ (**) or $p < 0.05$ (*). (D) Drought tolerance assays of Col-0, *skip5-1, skip5-2*, OE1 and OE2 plants. The photographs were taken 3 days after rehydration. (E) Survival rates of plants treated as described in (D). Survival rates were recorded 3 days after rehydration. Error bars are SD of three biological replicates, each consisting of at least 48 plants from 12 pots. Statistical analysis was performed by two-tailed Student's *t* test using GraphPad Prism v. 8.0.1, and asterisk represents significant differences at $p < 0.01$ (**). (F) Infrared thermography of seedlings from Col-0, *skip5-1, skip5-2*, OE1 and OE2. The graph shows the leaf temperature measured using infrared camera software. (G) RT-qPCR analysis of the expression levels of *AtSKIP5* in Col-0 under normal (Mock) and drought stress. Error bars are SD of three biological replicates. Asterisks indicate significant differences by two-tailed Student's *t* test using GraphPad Prism v. 8.0.1 at $p < 0.01$ (**). (H) Fresh weights of the detached leaves of seedlings from Col-0, *skip5-1, skip5-2*, OE1 and OE2 were measured at the indicated times. Error bars are SD of three biological replicates.

analysis of the survival rates revealed that the survival of the *skip5* mutants was lower than that of Col-0 plants, but the survival rates of the *AtSKIP5*-overexpressing lines were similar to that of Col-0 (Figure 7E). Furthermore, the gene expression levels of *AtSKIP5* in Col-0 under normal (mock) conditions and drought stress over a 2-week period were determined using RT-qPCR. The expression level of the *AtSKIP5* gene significantly increased under drought treatment compared to the mock conditions (Figure 7G). These results suggested that AtSKIP5 serves as a positive regulator in terms of drought tolerance. When water is deficient, plants respond to this drought stress by closing the stomata to prevent transpiration and thus water loss. An infrared camera was used to determine the transpiration rates of shoots; the leaf temperatures of 5-week-old plants were measured. There was no significant difference in leaf temperatures between the Col-0 and the *AtSKIP5*-overexpressing lines. However, the leaf temperatures were significantly lower for the *skip5* mutants than for Col-0 (Figure 7F). Water loss from Col-0 and *skip5* mutants rosette leaves of 5-week-old plants was measured during incubation at 22°C under light. As shown in Figure 7H, the rate of water loss was significantly greater in the *skip5* mutants than in the Col-0 and *AtSKIP5*-overexpressing lines (Figure 7H). These results showed that AtSKIP5 contributed to drought tolerance by promoting stomatal closure, preventing transpiration and water loss in *Arabidopsis*.

3 | Discussion

In this study, we explored the functions of the F-box protein AtSKIP5 in *Arabidopsis*; this guard cell protein is involved in resistance to Pst DC3000 infection and drought tolerance by regulating stomatal movement. Our results shed light on the link between stomatal responses to pathogen and drought stresses, with stomatal movement as a central hub, mediated by AtSKIP5; the stomatal closure triggered by various stimuli is similar.

AtSKIP5 is a member of the subfamily of AtSKIPs, which bind to the Skp1/ASK1 component. Importantly, the Y2H and BiFC assays revealed that AtSKIP5 indeed interacted with the AtASK1 protein, suggesting that AtSKIP5 exhibits a key characteristic of the AtSKIPs. The *skip5* mutants were more susceptible to Pst DC3000 infection, but the OE1 and OE2 lines were more resistant, suggesting that AtSKIP5 serves as a positive regulator of resistance to the bacterium Pst DC3000. The stomatal aperture assay revealed that AtSKIP5 played a positive role in the response to bacteria by controlling stomatal immunity via positively regulating flg22-triggered stomatal closure and suppressing COR-mediated stomatal reopening. Supporting these roles in stomata, the location analyses revealed that AtSKIP5 was expressed in guard cells (Figure 2). Known regulators involved in the stomatal immunity response include the lectin receptor kinase family, TFs and elicitor peptides (Chan et al. 2020; Zheng et al. 2018; Song et al. 2022). This study has thus increased the number of stomatal immunity players and suggests that the E3 Ub ligase plays a role in the stomatal responses to bacteria. In terms of the other proteins expressed in guard cells, as shown in Figure 1B, it might be interesting to explore whether these AtSKIPs, besides AtSKIP5, are also involved in the stomatal response, which could help to determine both the common and the unique functions amongst AtSKIPs. OE2 exhibited weaker bacterial-induced symptoms and stronger stomatal movements under different stress conditions than did OE1. We speculate that overexpressed AtSKIP5 protein may undergo post-translational modification or other unknown changes that may explain the higher transcriptional activity and protein expression of OE2 compared to OE1. The gene expression level of *AtSKIP5* in OE2 was higher than that in OE1, as revealed by both RT-qPCR and western blotting, supporting our speculation. *AtSKIP5* expression still increased from 4 to 24 h after dip-inoculation with Pst DC3000, implying that less efficient stomatal closure and inhibition of COR-dependent stomatal reopening are not the only reasons why the Pst DC3000 dip-inoculation resistance phenotype of these *skip5* mutants was compromised. Zeng et al. distinguished the contributions made by different host cell types in response to an infection and divided susceptible to *coronatine-deficient* Pst DC3000 (*scord*) mutants into three categories: deficient in terms of stomatal defence, deficient in terms of apoplastic defence, and deficient in terms of both stomatal and apoplastic defence (Zeng et al. 2011). Similar to the *scord1*, *-3*, *-6*, and *-8* mutants, the *skip5* mutants were more susceptible to bacteria either by dip inoculation or infiltration. Moreover, the *skip5* mutants were more susceptible to bacteria not only in terms of the basal apoplastic defence but also the apoplastic defence induced by flg22, as evidenced by the weaker ROS burst, lower MAPK phosphorylation level, and less callose deposition than Col-0 plants treated with flg22. Taken together, these data suggest that AtSKIP5 enhances *Arabidopsis* defences by restricting bacterial entry into leaves early in infection by redeploying host cells to ensure rapid strengthening of cell walls, and by activating ROS production and MAPK phosphorylation to suppress pathogen growth. AtSKIP5 was expressed in true leaves, suggesting that its expression in other cell types, besides guard cells, may fulfil additional functions, such as mediating ROS burst, MAPK phosphorylation, and callose deposition. Similarly, SIF2, a protein mainly expressed in guard cells, exhibited a basal level of expression in mesophyll cells, contributing to bacterial resistance through apoplastic mechanisms in *Arabidopsis* (Chan et al. 2020). An unexpected finding is that mutation of AtSKIP5 impaired callose deposition but did not affect the expression levels of *FRK1* and *CYP81F2*. Similar results were reported previously. SIF2 did not affect the expression levels of *FRK1* or *CYP81F2* but was nonetheless involved in callose deposition during the late apoplastic PTI response (Chan et al. 2020). In view of these findings, we speculate that either the expression levels of *FRK1* and *CYP81F2* exhibit drastic changes associated with a response induced by PAMP/MAMPs rather than directly by Pst DC3000 infection, or the role of AtSKIP5 in apoplastic defence does not involve an FRK1- and CYP81F2-mediated regulatory mechanism. Plants use ROS as versatile signalling molecules to respond rapidly and appropriately to pathogen challenge. Plants tightly regulate the activation and deactivation of RBOHs, key enzymes in ROS production that are localised at the plasma membrane, through various post-translational modifications, including ubiquitination (Xu and Xue 2019; Yan et al. 2024). It has been reported that the E3 Ub ligase PIRE ubiquitinates RBOHD to negatively regulate the ROS burst (Lee et al. 2020). In this study, AtSKIP5 was a component of the SCF E3 ubiquitin ligase complex and was involved in the ROS burst MAPK phosphorylation upon flg22 treatment. Given the role of E3 ubiquitin ligases in the ROS burst, it might be that AtSKIP5 is involved in the specific recognition of substrates involved in this process, such as RBOHs, as well as in other early immune signalling processes. Further screening

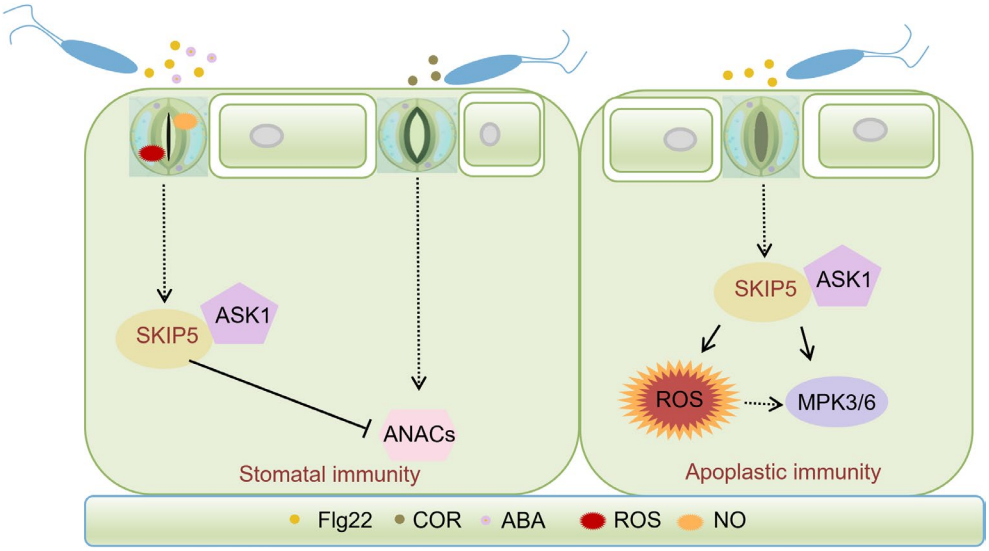

FIGURE 8 | A proposed model for that AtSKIP5 positively regulates plant immunity and drought tolerance by stomatal movement in *Arabidopsis*.

and identification of the AtSKIP5 substrates involved in these physiological processes could enhance our understanding of the mechanisms by which AtSKIP5 contributes to plant immunity.

ABA is the best-studied hormone that regulates plant tolerance to drought and stomatal closure (Guzman et al. 2012; Jossier et al. 2009). In our study, AtSKIP5 expression gradually rose as the ABA treatment time increased. Moreover, AtSKIP5 was required for ABA-induced stomatal closure, indicating that the function of AtSKIP5 is associated with stomatal movement mediated by ABA signalling. The expression level of *AtSKIP5* was high under drought conditions, and the *skip5* mutants were more sensitive to drought than was Col-0 based on a comparison of the survival rates, suggesting that AtSKIP5 positively regulates drought tolerance by promoting stomatal closure mediated by ABA signalling. Prevention of leaf water loss is an important drought tolerance mechanism (Tian et al. 2022). Consistent with these results, AtSKIP5 inhibited leaf water loss and increased the leaf temperature, suggesting that the transpiration rates of *skip5* mutant plants were higher than that of Col-0. Together, these results suggest a role for AtSKIP5 in terms of control of guard cell water status to promote stomatal closure and thus enhance drought tolerance in *Arabidopsis*. In *Arabidopsis*, stomatal closure mediated by ABA aids the plant defence against Pst DC3000 infection. Under drought stress, stomatal closure by ABA may also enhance plant drought tolerance by inhibiting leaf water loss and decreasing the transpiration rate. This study showed that AtSKIP5 was involved in the resistance to Pst DC3000 by regulating stomatal closure, and it played a positive role in drought tolerance mediated by ABA-induced stomatal closure, implying that AtSKIP5-mediated resistance to Pst DC3000 may be associated with ABA signalling.

In conclusion, we propose a working model of the possible mechanism by which the F-box protein AtSKIP5 regulates plant immunity and drought tolerance by controlling stomatal responses (Figure 8). When a plant senses Pst DC3000 or PAMP (flg22), it activates AtSKIP5, which triggers rapid stomatal closure and ROS and NO production in guard cells to restrict bacterial entry into leaves. To successfully colonise plants, Pst DC3000 produces the toxin COR to reopen closed stomata. AtSKIP5 suppresses COR-induced stomatal reopening by promoting protein degradation of *ANAC019*, *ANAC055*, and *ANAC072*. Even if Pst DC3000 overcomes the surface barrier and enters the interior spaces of leaves, AtSKIP5 still suppresses bacterial growth by activating ROS production and MAPK phosphorylation induced by flg22. In addition, both ABA and the drought-induced increase in ABA levels activate the expression of AtSKIP5, followed by stomatal closure, thus increasing drought tolerance. AtSKIP5 is a component of the SCF E3 Ub ligases. Based on the above results, AtSKIP5-mediated stomatal movement may be affected by ubiquitination, needing to be confirmed by further study.

4 | Experimental Procedures

4.1 | Plant Material and Growth Conditions

The *Arabidopsis* transgenic lines used in this study are in the Columbia (Col-0) background. The *skip5-1* mutant (SALK_055942 in a Col-0 background) and *skip5-2* mutant (SALK_044720 in a Col-0 background) were obtained from the Arabidopsis Biological Resource Center (https://abrc.osu.edu). *Arabidopsis* plants were grown in commercial potting soil with perlite in a 3:2 ratio, at 22°C, under 80 $mmol^{-2}$ m^{-2} s^{-1} illumination using bulb-type fluorescent light with a 12-h light/night and a 10-h light/14-h dark photoperiod.

4.2 | Plasmid Construction and Plant Transformation

To generate *AtSKIP5* overexpression lines, the full-length coding sequences of the *AtSKIP5* gene were cloned into the pCN-GFP vector under the control of the CaMV 35S promoter via recombination-based cloning as described in our previous

study (Song et al. 2022). All constructs were transformed into *Arabidopsis* Col-0 plants using the *Agrobacterium tumefaciens* GV3101-mediated floral dip method (Clough and Bent 1998). Lines stably expressing the *AtSKIP5* transcript and protein were used in subsequent experiments.

4.3 | Subcellular Localisation of AtSKIP5

To observe the localisation of AtSKIP5, the coding sequence of AtSKIP5 was cloned into the pUC19-GFP and pBINPLUS-GFP vectors. The pUC19-AtSKIP5-GFP construct (driven by the 35S promoter) was transformed into *Arabidopsis* mesophyll protoplasts according to a previously described protocol (Yoo et al. 2007). The pBINPLUS-AtSKIP5-GFP plasmid in *A. tumefaciens* GV3101 was infiltrated into fully expanded leaves of 5-week-old *N. benthamiana* plants. The resulting transformants were observed under a confocal fluorescence microscope (AX; Nikon).

4.4 | Y2H Assay and BiFC Assay

The Y2H experiments were performed as previously described by Chan et al. (2020). Full-length coding fragments of *AtASK1* were cloned into the GAL4 activation plasmid (pGADT7), and full-length coding fragments of *AtSKIP5* were cloned into the GAL4 binding plasmid (pGBKT7) using restriction enzyme-mediated ligation, respectively. Protein–protein interactions were determined by growing the co-transformed yeast strains on SD/−Ade/−His/−Trp/−Leu (SD − A/H/T/L) medium for 4 days at 30°C. The BiFC experiments were performed in *N. benthamiana* leaves as previously described in the method (Chan et al. 2020). The full-length coding fragments of *AtASK1* and *AtSKIP5* were cloned into the split-YFP destination vectors (YN and YC), respectively. The constructs were transformed into *A. tumefaciens* EHA105 and co-infiltrated into leaves. After 48 h, the resulting transformants were observed under a confocal fluorescence microscope (AX; Nikon).

4.5 | Pst DC3000 Infection Assay

Pst DC3000 was cultured in King's B medium with kanamycin at 28°C. For dipping inoculation, the bacteria were resuspended in sterile 10 mM $MgCl_2$ buffer to 10^7 cfu/mL after centrifugation. Silwet L-77 was added to the bacterial suspension to 0.02% (vol/vol) immediately before dipping. Five-week-old plants were dip-inoculated for 3 min in bacterial suspensions and then kept at 100% relative humidity for one night. For syringe inoculation, the bacteria were resuspended in 10 mM $MgCl_2$ to a concentration of 10^5 cfu/mL and infiltrated using a needleless syringe into leaves. Diseased leaves were photographed after 4 days. Bacterial titres were quantified on King's B agar plates as described previously (Zimmerli et al. 2000).

4.6 | Stomatal Aperture Assay

Stomatal assays followed procedures described in a previous study (Zeng et al. 2011; Song et al. 2022). Fully expanded leaves of 5-week-old plants were floated on stomatal buffer (50 mM KCl, 50 μM $CaCl_2$, 10 mM MES-Tris, pH 6.15) and kept under light for at least 2 h to open stomata before the beginning of the experiments. The 1 μM flg22, 10 μM ABA, bacteria (10^8 cfu/mL), and 2 μM COR were then added at the indicated time. The peels were mounted on microscope slides and imaged at the indicated time points with a microscope (ECLIPSE Ti2; Nikon). The length and width of the stomatal aperture were measured using ImageJ (Media Cybernetic).

4.7 | Western Blot Assays and MAP Kinase Assay

Protein extraction was performed as described previously (Yeh et al. 2016). In brief, the powder of young leaves from 5-week-old *Arabidopsis* was transferred to a 2 mL tube and mixed with 0.5 mL extraction buffer (50 mM Tris–HCl pH 7.4, pH 7.5, 150 mM NaCl, 2 mM EDTA, Triton X-100, 1% [vol/vol] Roche protease inhibitor cocktail). After agitating three times, supernatants were collected as total proteins by centrifugation at 10,000 *g* for 10 min at 4°C. Protein concentration was quantified using the bicinchoninic acid (BCA) Protein Assay Kit (Solarbio). Proteins were separated by 10% SDS-PAGE and detected by immunoblotting using appropriate antibodies. MAP kinase assay was performed as described previously (Singh et al. 2012).

4.8 | Quantification of Gene Expression by RT-qPCR

RT-qPCR assays were performed as described in a previous study (Vogels et al. 2020). Total RNA samples were extracted from 5-week-old leaves under normal conditions and drought stress over a 2-week period using the RNAsimple Total RNA Kit (Tiangen) according to the manufacturer's protocol. Reverse transcription was performed using a PrimeScript RT reagent kit (TaKaRa). RT-qPCR was run on a CFX Duet Real-Time PCR system (Bio-Rad) with SYBR Premix ExTaq (Vazyme Biotech). The relative quantification of each transcript was calculated by the $2^{-\Delta\Delta Ct}$ method (Livak and Schmittgen 2001). For each gene, the RT-qPCR assay was repeated three times with three biological replicates. The primers used in this section are listed in Table S1.

4.9 | ROS Burst and Callose Deposition

ROS assays were performed as previously described (Song et al. 2022). Briefly, 10 mm diameter of 12 leaf discs from 5-week-old *Arabidopsis* were incubated in double-distilled water in 96-well plates overnight. The following day, the water was replaced by 100 nM flg22 in 10 mM $MgSO_4$ buffer or by 10 mM $MgSO_4$ buffer only for the mock controls containing 20 mM luminol (Sigma-Aldrich) and 10 mg/mL peroxidase (Sigma-Aldrich). Luminescence was measured using a luminometer (Berthold Technologies). The callose deposition assay was performed as described previously (Chan et al. 2020). Leaves from 5-week-old *Arabidopsis* were infiltrated with 1 μM flg22 and with double-distilled water only for the mock controls. Cleared leaf discs were stained with 0.01% (wt/vol) aniline blue in 0.15 M phosphate buffer, pH 9.5, for 4 h. Callose deposits were visualised under UV light illumination using a microscope (Eclipse Ti2; Nikon). Quantification of callose deposits was performed on the acquired digital images using ImageJ.

4.10 | Monitoring of ROS and NO in Guard Cells

ROS and NO levels in guard cells were detected as previously described (Liu et al. 2011; Song et al. 2022; He et al. 2022). To quantify ROS and NO levels, epidermal peels, devoid of mesophyll cells, dipped into stomatal buffer with or without 1 μM flg22, were stained with H_2DCF-DA (50 mM) or DAF-2DA (50 mM), respectively. After 30 min of incubation in the dark at 25°C, the excess dye on the epidermal peels was washed with buffer, and fluorescence was observed with a fluorescence microscope.

4.11 | Water Loss Assay and Drought Treatment

For a water loss assay with detached leaves, rosette leaves were cut from 5-week-old plants in soil. The weight of the detached leaves was measured every 1 h over about 4 h at 22°C, as previously described (Dou et al. 2021; Yu et al. 2020). Water loss was represented as the percentage of initial fresh weight at each time point. For drought treatment, plants were grown in vermiculite for 14 days with sufficient watering, followed by 14 days of drought stress and then rewatered for 3 days. All plants were grown in a small pot under a 12-h light/dark photoperiod at 22°C, as previously described (Dou et al. 2021; Meng et al. 2024).

4.12 | Statistical Analysis

Statistical analysis was performed with Graphpad Prism v. 8.0.1. Two-tailed Student's *t* test and one-way ANOVA were used to analyse data. The significance of differences between samples was statistically evaluated using SD or SE.

Acknowledgements

This work was supported in part by the National Natural Science Foundation of China (grants 32472531, 32302304 and 32072366).

Conflicts of Interest

The authors declare no conflicts of interest.

Data Availability Statement

All relevant data can be found within the manuscript and its supporting materials.

References

Agurla, S., S. Gahir, S. Munemasa, Y. Murata, and A. S. Raghavendra. 2018. "Mechanism of Stomatal Closure in Plants Exposed to Drought and Cold Stress." *Advances in Experimental Medicine and Biology* 1081: 215–232.

Arnaud, D., M. J. Deeks, and N. Smirnoff. 2023. "RBOHF Activates Stomatal Immunity by Modulating Both Reactive Oxygen Species and Apoplastic pH Dynamics in *Arabidopsis*." *Plant Journal* 116: 404–415.

Chan, C., D. Panzeri, E. Okuma, et al. 2020. "STRESS INDUCED FACTOR 2 Regulates *Arabidopsis* Stomatal Immunity Through Phosphorylation of the Anion Channel SLAC1." *Plant Cell* 32: 2216–2236.

Chen, C., H. Chen, Y. Zhang, et al. 2020. "TBtools: An Integrative Toolkit Developed for Interactive Analyses of Big Biological Data." *Molecular Plant* 13: 1194–1202.

Clough, S. J., and A. F. Bent. 1998. "Floral Dip: A Simplified Method for *Agrobacterium*-Mediated Transformation of *Arabidopsis thaliana*." *Plant Journal* 16: 735–743.

David, L., A. C. Harmon, and S. Chen. 2019. "Plant Immune Responses—From Guard Cells and Local Responses to Systemic Defense Against Bacterial Pathogens." *Plant Signaling & Behavior* 14: e1588667.

Ding, S., B. Zhang, and F. Qin. 2015. "*Arabidopsis* RZFP34/CHYR1, a Ubiquitin E3 Ligase, Regulates Stomatal Movement and Drought Tolerance via SnRK2.6-Mediated Phosphorylation." *Plant Cell* 27: 3228–3244.

Doehlemann, G., and C. Hemetsberger. 2013. "Apoplastic Immunity and Its Suppression by Filamentous Plant Pathogens." *New Phytologist* 198: 1001–1016.

Dou, L., K. He, J. Peng, X. Wang, and T. Mao. 2021. "The E3 Ligase MREL57 Modulates Microtubule Stability and Stomatal Closure in Response to ABA." *Nature Communications* 12: 2181.

Du, M., Q. Z. Zhai, L. Deng, et al. 2014. "Closely Related NAC Transcription Factors of Tomato Differentially Regulate Stomatal Closure and Reopening During Pathogen Attack." *Plant Cell* 26: 3167–3184.

Gautam, V., and A. K. Sarkar. 2015. "Laser Assisted Microdissection, an Efficient Technique to Understand Tissue Specific Gene Expression Patterns and Functional Genomics in Plants." *Molecular Biotechnology* 57: 299–308.

Guo, H. Q., T. M. Nolan, G. Y. Song, et al. 2018. "FERONIA Receptor Kinase Contributes to Plant Immunity by Suppressing Jasmonic Acid Signaling in *Arabidopsis thaliana*." *Current Biology* 28: 3316–3324.

Guzman, M., G. A. Pizzio, R. Antoni, et al. 2012. "*Arabidopsis* PYR/PYL/RCAR Receptors Play a Major Role in Quantitative Regulation of Stomatal Aperture and Transcriptional Response to Abscisic Acid." *Plant Cell* 24: 2483–2496.

He, N. Y., L. S. Chen, A. Z. Sun, Y. Zhao, S. N. Yin, and F. Q. Guo. 2022. "A Nitric Oxide Burst at the Shoot Apex Triggers a Heat-Responsive Pathway in *Arabidopsis*." *Nature Plants* 8: 434–450.

Hirofumi, K., T. Naoki, S. Hiroaki, S. Motoaki, S. Kazuo, and M. Minami. 2002. "Classification and Expression Analysis of *Arabidopsis* F-Box Containing Protein Genes." *Plant & Cell Physiology* 43: 1073–1085.

Hong, J. P., E. Adams, Y. Yanagawa, M. Matsui, and R. Shin. 2017. "AtSKIP18 and AtSKIP31, F-Box Subunits of the SCF E3 Ubiquitin Ligase Complex, Mediate the Degradation of 14-3-3 Proteins in *Arabidopsis*." *Biochemical and Biophysical Research Communications* 485: 174–180.

Jennifer, M. G., P. D. Brian, H. S. Shin, M. D. Adam, and D. V. Richard. 2002. "The F-Box Subunit of the SCF E3 Complex Is Encoded by a Diverse Superfamily of Genes in *Arabidopsis*." *Proceedings of the National Academy of Sciences of the United States of America* 29: 11519–11524.

Jossier, M., J. P. Bouly, P. Meimoun, et al. 2009. "SnRK1 (SNF1-Related Kinase 1) has a Central Role in Sugar and ABA Signalling in *Arabidopsis thaliana*." *Plant Journal* 59: 316–328.

Lee, D., N. K. Lal, Z. D. Lin, et al. 2020. "Regulation of Reactive Oxygen Species During Plant Immunity Through Phosphorylation and Ubiquitination of RBOHD." *Nature Communications* 11: 1838.

Li, J. J., Y. Li, Z. G. Yin, et al. 2016. "OsASR5 Enhances Drought Tolerance Through a Stomatal Closure Pathway Associated With ABA and H_2O_2 Signalling in Rice." *Plant Biotechnology Journal* 15: 183–196.

Li, Y., L. Zhang, D. K. Li, et al. 2015. "The *Arabidopsis* F-Box E3 Ligase RIFP1 Plays a Negative Role in Abscisic Acid Signalling by Facilitating ABA Receptor RCAR3 Degradation." *Plant, Cell and Environment* 39: 571–582.

Liu, D., Z. Chen, P. Shi, X. Wang, and W. Cai. 2011. "Analysis of Reactive Oxygen Species in the Guard Cell of Wheat Stoma With Confocal Microscope." *Microscopy Research and Technique* 74: 795–798.

Livak, K. J., and T. D. Schmittgen. 2001. "Analysis of Relative Gene Expression Data Using Real-Time Quantitative PCR and the $2^{-\Delta\Delta CT}$ Method." *Methods* 25: 402–408.

Melotto, M., W. Underwood, J. Koczan, K. Nomura, and S. Y. He. 2006. "Plant Stomata Function in Innate Immunity Against Bacterial Invasion." *Cell* 126: 969–980.

Meng, Y., Q. Lv, L. Q. Li, et al. 2024. "E3 Ubiquitin Ligase TaSDIR1-4A Activates Membrane-Bound Transcription Factor TaWRKY29 to Positively Regulate Drought Resistance." *Plant Biotechnology Journal* 22: 987–1000.

Mez, L. G., and T. Boller. 2000. "FLS2: An LRR Receptor-Like Kinase Involved in the Perception of the Bacterial Elicitor Flagellin in *Arabidopsis*." *Molecular Cell* 5: 1003–1011.

Monaghan, J., and C. Zipfel. 2012. "Plant Pattern Recognition Receptor Complexes at the Plasma Membrane." *Current Opinion in Plant Biology* 15: 349–357.

Naeem-ul-Hassan, M., Z. Zainal, C. J. Kiat, H. H. Monfared, and I. Ismail. 2017. "*Arabidopsis thaliana* SKP1 Interacting Protein 11 (At2g02870) Negatively Regulates the Release of Green Leaf Volatiles." *Royal Society of Chemistry Advances* 7: 55725–55733.

Penninckx, I., B. Thomma, B. Antony, P. M. Jean, and F. B. Willem. 1998. "Concomitant Activation of Jasmonate and Ethylene Response Pathways Is Required for Induction of a Plant Defensin Gene in *Arabidopsis*." *Plant Cell* 10: 2103–2113.

Rao, V., B. P. Petla, P. Verma, et al. 2018. "*Arabidopsis* SKP1-Like protein13 (ASK13) Positively Regulates Seed Germination and Seedling Growth Under Abiotic Stress." *Journal of Experimental Botany* 69: 3899–3915.

Shen, C., Y. Zhang, Q. Li, et al. 2021. "PdGNC Confers Drought Tolerance by Mediating Stomatal Closure Resulting From NO and H_2O_2 Production via the Direct Regulation of PdHXK1 Expression in *Populus*." *New Phytologist* 230: 1868–1882.

Sierla, M., C. Waszczak, T. Vahisalu, and J. Kangasjärvi. 2016. "Reactive Oxygen Species in the Regulation of Stomatal Movements." *Plant Physiology* 171: 1569–1580.

Singh, P., Y. C. Kuo, S. Mishra, et al. 2012. "The Lectin Receptor Kinase-VI.2 Is Required for Priming and Positively Regulates *Arabidopsis* Pattern-Triggered Immunity." *Plant Cell* 24: 1256–1270.

Song, Z., C. Zhang, P. Y. Jin, et al. 2022. "The Cell-Type Specific Role of *Arabidopsis* bZIP59 Transcription Factor in Plant Immunity." *Plant, Cell and Environment* 45: 1843–1861.

Spoel, S. H., and X. Dong. 2008. "Making Sense of Hormone Crosstalk During Plant Immune Responses." *Cell Host and Microbe* 3: 348–351.

Su, J. B., M. M. Zhang, L. Zhang, et al. 2017. "Regulation of Stomatal Immunity by Interdependent Functions of a Pathogen-Responsive MPK3/MPK6 Cascade and Abscisic Acid." *Plant Cell* 29: 526–542.

Tian, H. T., Y. Watanabe, K. H. Nguyen, et al. 2022. "*KARRIKIN UPREGULATED* F-Box 1 Negatively Regulates Drought Tolerance in *Arabidopsis*." *Plant Physiology* 190: 2671–2687.

Varshney, V., A. Hazra, V. Rao, et al. 2023. "The *Arabidopsis* F-Box Protein *SKP1-INTERACTING PARTNER* 31 Modulates Seed Maturation and Seed Vigor by Targeting *JASMONATE ZIM DOMAIN* Proteins Independently of Jasmonic Acid-Isoleucine." *Plant Cell* 35: 3712–3738.

Vogels, C. B. F., A. F. Brito, A. L. Wyllie, et al. 2020. "Analytical Sensitivity and Efficiency Comparisons of SARS-CoV-2 RT-qPCR Primer-Probe Sets." *Nature Reviews Microbiology* 5: 1299–1305.

Wang, Z., and X. Q. Gou. 2021. "The First Line of Defense: Receptor-Like Protein Kinase-Mediated Stomatal Immunity." *International Journal of Molecular Sciences* 23: 343.

Xu, F. Q., and H. W. Xue. 2019. "The Ubiquitin-Proteasome System in Plant Responses to Environments." *Plant, Cell and Environment* 42: 2931–2944.

Yan, J., C. Zhang, M. Gu, et al. 2009. "The *Arabidopsis* CORONATINE INSENSITIVE1 Protein Is a Jasmonate Receptor." *Plant Cell* 21: 2220–2236.

Yan, Y., H. Wang, Y. Bi, and F. Song. 2024. "Rice E3 Ubiquitin Ligases: From Key Modulators of Host Immunity to Potential Breeding Applications." *Plant Communications* 5: 101128.

Yeh, Y. H., D. Panzeri, Y. Kadota, et al. 2016. "The *Arabidopsis* Malectin-Like/LRR-RLK IOS1 Is Critical for BAK1-Dependent and BAK1-Independent Pattern-Triggered Immunity." *Plant Cell* 28: 1701–1721.

Yoo, S. D., Y. H. Cho, and J. Sheen. 2007. "*Arabidopsis* Mesophyll Protoplasts: A Versatile Cell System for Transient Gene Expression Analysis." *Nature Protocols* 2: 1565–1572.

Yu, S. G., J. H. Kim, N. H. Cho, T. R. Oh, and W. T. Kim. 2020. "*Arabidopsis* RING E3 Ubiquitin Ligase JUL1 Participates in ABA-Mediated Microtubule Depolymerization, Stomatal Closure, and Tolerance Response to Drought Stress." *Plant Journal* 103: 824–842.

Zeng, W., A. Brutus, J. M. Kremer, et al. 2011. "A Genetic Screen Reveals *Arabidopsis* Stomatal and/or Apoplastic Defenses Against *Pseudomonas syringae* pv. *tomato* DC3000." *PLoS Pathogens* 7: e1002291.

Zhang, Y. E., W. Y. Xu, Z. H. Li, X. W. Deng, W. H. Wu, and Y. B. Xue. 2008. "F-Box Protein DOR Functions as a Novel Inhibitory Factor for Abscisic Acid-Induced Stomatal Closure Under Drought Stress in *Arabidopsis*." *Plant Physiology* 148: 2121–2133.

Zheng, X., S. Kang, Y. Jing, et al. 2018. "Danger-Associated Peptides Close Stomata by OST1-Independent Activation of Anion Channels in Guard Cells." *Plant Cell* 30: 1132–1146.

Zimmerli, L., G. Jakab, J. P. Me´ traux, and B. Mauch. 2000. "Potentiation of Pathogen-Specific Defense Mechanisms in *Arabidopsis* by β-Aminobutyric Acid." *Proceedings of the National Academy of Sciences of the United States of America* 97: 12920–12925.

Supporting Information

Additional supporting information can be found online in the Supporting Information section.